MICRO-ROTATION IMAGING DECONVOLUTION

B. Le Saux, B. Chalmond, Y. Yu, A. Trouvé

CMLA
ENS Cachan, CNRS, UniverSud
61 Avenue Président Wilson
Cachan 94230, France
{lesaux, chalmond, yu, trouve}@cmla.ens-cachan.fr

O. Renaud, S.L. Shorte

Plateforme d'Imagerie Dynamique (PFID)
Imagopole, Institut Pasteur
25-28 rue du Dr. Roux
Paris 75015, France
{orenaud, sshorte}@pasteur.fr

ABSTRACT

Recently, micro-rotation confocal microscopy has enabled the acquisition of a sequence of slices of non adherent living cells obtained during a partially controlled rotation movement of the cell through the focal plane. Although we are now able to estimate the 3D position of every slice with respect to the frame, the reconstruction of the cell from the positioned slices remains a problem that this paper address. In our context, 3D spatially-varying PSF and missing data are the two main particularities of this problem. Experiments illustrate the ability of the classical EM algorithm to deconvolve efficiently cell volume and also to deal with missing data.

Index Terms— Micro-rotation confocal microscopy, deconvolution, interpolation, 3D spatially-varying PSF, missing data, non-organized data.

1. INTRODUCTION

Our microscope is equipped with a di-electrophoretic field control microelectrode cage which enables trapping of non adherent living cells [1, 2, 3]. Once a cell has been trapped, it undergoes continuous unstable rotations around a main axis [4]. During the rotation, a sequence of microscopic images $(S^k)_{1\leq k\leq N}$ is obtained through the fixed focal plane F at a given rate. Each image is taken under the same microscopic conditions. Fig.2 (first column) shows four images extracted from a sequence of 340 slices per turn of a cell in rotation. Among the advantages of such an apparatus, is the ability to alleviate the problem of anisotropy of the microscope resolution : the resolution perpendicular to the focal plane is half of the resolution within the focal plane [**?**]. That is translated into the microscope PSF which is mainly elongated along the z-axis.

Since the images are all recorded in the fixed plane F, their positions inside the cell are unknown. However, these positions can be estimated using the method presented in [5]. So, here, we assume that the images have been aligned according to these positions. The situation where the cell is rotating and F is fixed is equivalent to the *dual* situation where the cell is fixed and F is rotating. Throughout these lines, we adopt the dual case. With this viewpoint, we understand that the PSF whose main axis is perpendicular to the focal plane, is spatially-varying : each image has its own oriented PSF. Another particularity arises from our microscope equipment. When F turns around an axis which is not included into it, a part of the 3D space is not covered by the moving plane. Since no data are captured in this area, a "black hole" is apparent in the 3D cell representation when this artefact is not treated (see Fig.3, column 1). The main contribution of this paper is to deal with the spatially-varying PSF and missing data.

In §2, we propose a geometric set-up to link the slices to the 3D cell volume and an algorithm to perform the 3D volume deconvolution. In §3 we show that the 3D deconvolution allows to dramatically improve the quality of the cross-sections, improve the quality of the volume reconstruction if compared to other attempts, and eventually allow under some given restrictions to interpolate the cell voxels when no data are available. Furthermore, contrary to many others propositions, our volume deconvolution does not use any regularization constraint. Finally we present our concluding remarks in §. 4.

2. MICRO-ROTATION IMAGE DECONVOLUTION

2.1. Spatially-varying PSF

Recall that we assume the cell is fixed and the focal plane is rotating. In fact, the focal plane is assimilated to a square grid, that is, the image acquisition grid. In a given frame $\mathcal{R}=(oxyz)$, let m be the unknown cell volume defined on a square 3D grid G, such that the reference focal plane F is contained in (oxy). F_k denotes the positions of the moving focal plane supporting the image S^k. When the focal plane is moving, the

shape of the PSF Ψ_k remains unchanged but its orientation changes according to the movement of the focal plane since the main axis of the PSF is always perpendicular to F_k. Computing 3D image convolution with such a varying PSF is quite calculation intensive. So, we use the following scheme which allows to use only the PSF Ψ associated to the reference focal plane F.

For every positioned focal plane F_k, let us define a 3D square grid G_k such that two faces are parallel to F_k and are at equal distance to F_k. The node values of G_k are obtained by interpolation from those of G :

$$m^k = A^k m \ , \tag{1}$$

where the interpolation operator A^k depends only on the geometric application between G and G_k. If H_k is the linear operator associated to the PSF Ψ_k, *with respect to the frame* G_k, we consider the model

$$\mathbf{E}[\mathbf{S}^k] = PHm^k \ , \tag{2}$$

where $\mathbf{S}^k$ is the random vector whose S^k is an occurrence. P is the slice operator $P : \mathbb{R}^{d^3} \longrightarrow \mathbb{R}^{d^2}$. Behind this formula is $\Psi_k \star m = \Psi \star m_k$. Finally, we get

$$\mathbf{E}[\mathbf{S}^k] = PHA^k m \ . \tag{3}$$

which modelizes the relationship between the data and the unknown volume. Below, we shall denote $\mathcal{H}^k = PHA^k$.

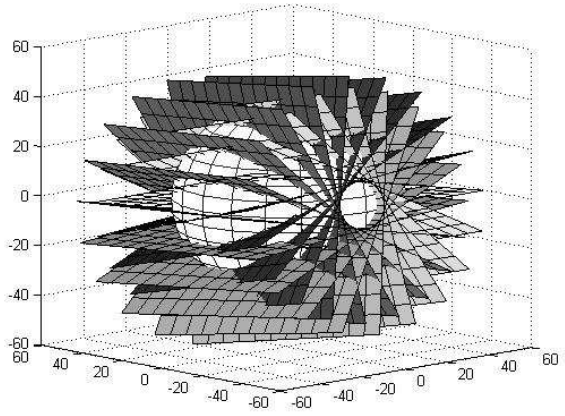

Fig. 1. Focal plane movement and black hole.

2.2. Deconvolution in the case of missing data

Image deconvolution is an old problem for which a well-known solution is given by the EM algorithm [6, 7]. Usually, in such a framework, the hidden variables m_i's have same locations than the observable variables. In this context, the EM algorithm is a means to formalize and stabilize the Lucy-Richardson algorithm [8, 9] rather than to deal with missing data. In our case, m is defined over the grid G which is larger than the data support $\mathcal{F} = \{F_k\}$ and furthermore some data are missing when a black hole is present. In this situation, the EM algorithm becomes completely justified and then we really take advantage of its property to deal with missing data [10]. Procedures for deconvoluting images in the case of non-organized and non-uniform data include the OS-EM algorithm [11].

Let us recall briefly the EM algorithm for deconvolution as introduced in [7]. For every site $i \in \mathcal{F}$ and $j \in G$, let x_{ij} be the number of photons received at i and coming from j. The observations are then given by $S_i^k = \sum_j x_{ij}$ and we assume that x_{ij} is the occurrence of a Poisson random variable $\mathcal{P}(\mathcal{H}_{ij}^k m_j)$. Under the hypothesis of independence, S_i^k is the occurrence of the Poisson random variable $\mathcal{P}(\sum_j \mathcal{H}_{ij}^k m_j)$.

From this model, we aim to find an estimate of m that maximizes the likelihood of $p(S|m)$. The general EM algorithm [6] works with the following expected log-likelihood

$$Q(m|m(t)) = \mathbf{E}\left[\log(p(x|m))|S, m(t)\right] \ , \tag{4}$$

with respect to the conditional distribution $p(x|S, m(t))$ where $m(t)$ is a current estimate. Starting with a given initial estimate $m(0)$, at each iteration t, one proves that the likelihood $p(S|m(t))$ increases.

By derivating expression (4), we find the classical update formula for a single voxel m_r, in which the PSF is in the micro-rotation case depending of its spatial position :

$$m_r(t+1) = m_r(t) \frac{\sum_{k,j} \mathcal{H}_{r,j}^k \frac{S_j^k}{\sum_l \mathcal{H}_{l,j}^k m_l(t)}}{\sum_{k,j} \mathcal{H}_{r,j}^k} \ .$$

By denoting $./$ the element-wise division and defining α so that $\alpha_i = \sum_{k,j} \mathcal{H}_{i,j}^k$, we can use matrix notation for the update step :

$$m(t+1) = (m(t)./\alpha) \sum_k (\mathcal{H}^k)^\top \left(S^k./(\mathcal{H}^k m(t))\right) \ .$$

Such a writing helps to implement the algorithm using the FFT, and thus allows acceptable computational times.

We have to emphasize that our deconvolution process does not integrate any regularization component. Since regularization is well known to be crucial to solve inverse problems (see [10, 12] among many others), in our firsts experiments, we have tested the role of regularization components and in particularly the total variation term as in [13]. But, on the light of the experimental results, we consider this regularization has no benefit effect for micro-rotation volume deconvolution.

3. EXPERIMENTS AND RESULTS

3.1. Data vs. estimate comparison

The first round of experiments aims to test the quality of the results. We compare the original data (slices obtained by the microscope) with slices in the estimate 3D images, taken at the same position. Results are shown in Fig. 2. The deconvolution process reveals details of the cell, like swellings or folds of the cell membrane.

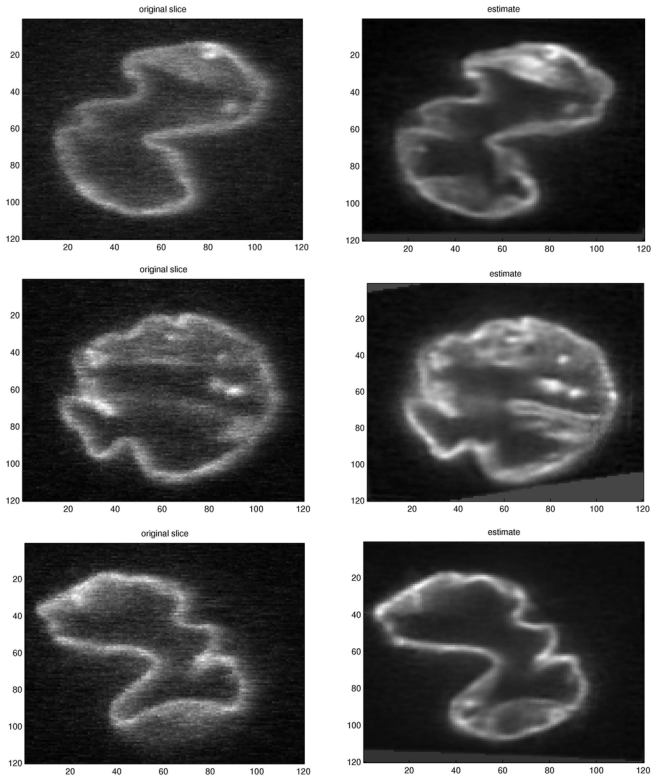

Fig. 2. Comparison of micro-rotation slices (first column) with the corresponding slice in the volume estimate (second column). The difference of view between two successive rows corresponds to a quarter-turn of the focal plane.

3.2. Comparison with other reconstruction method

In this round of experiments, we compare our results with the estimate obtained by another approach [5]. This reconstruction method is obtained with Gaussian kernels and does not deal with the PSF problem. The advantage of our approach is two-fold. First, more details are visible, which is the expected result of the deconvolution. Second, our approach has an interpolation effect that deals with the missing data. On some views of the left column of Fig. 3, a black hole is visible. Such an artefact occurs when the focal plane turns around an axis that is not included in it : part of the 3D space (which has the shape of a cone) is not covered by the moving plane. Since no data are captured in this area, the simple interpolation approach replaces it by a black hole. On the contrary, the deconvolution approach uses the PSF to propagate information and find an estimate of the voxel values at those locations (and thus fill the black hole).

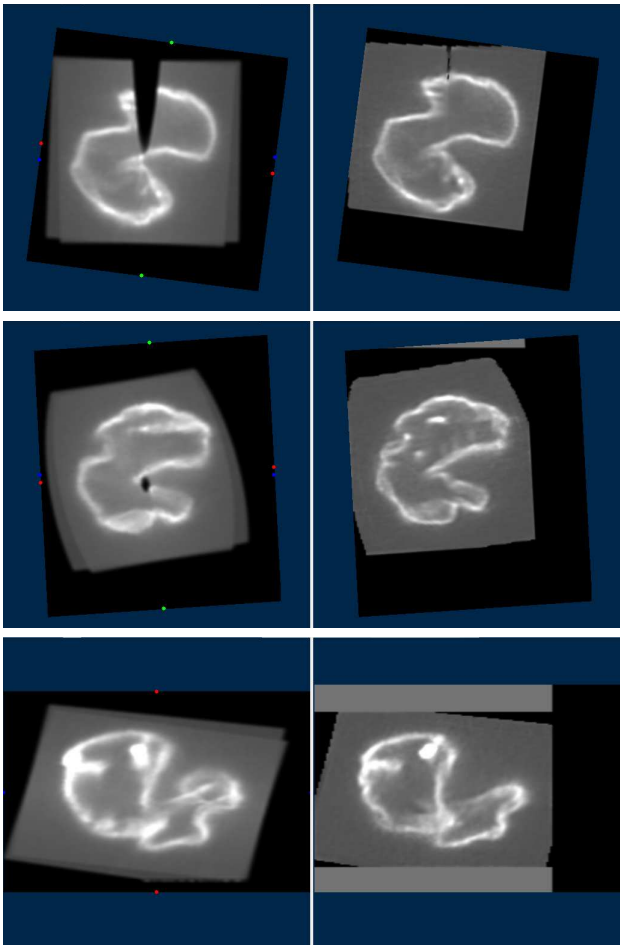

Fig. 3. Comparison of two reconstruction methods. Slices on the left are taken from the volume obtained by interpolation with Gaussian kernels. Slices on the right are taken from the volume obtained by the EM deconvolution process.

4. CONCLUSION

Deconvolution of micro-rotation image series, as presented here, yields a striking improvement in data quality including a strong reduction in 2D out-of-focus blur. This is due to efficient 3D light reconstruction whereby the PSF geometry and pitch orientation guides accurate 3D reassignment of out-of-focus light emanating from fluorescent features of interest. A most unexpected observation, and apparently peculiar to this novel imaging modality is the remarkable efficacy

of light reconstruction by deconvolution. We show that in the case where information is lost in micro-rotation feature reconstruction due mainly to incomplete sampling near the rotation axis (i.e. the black-hole artefact) that such information is fully recovered by the deconvolution process. This novel interpolation effect presumably arises due to the rotating PSF, and to our knowledge has yet to be characterized. Further, we find the counter-intuitive result whereby regularisation as total variation does not yield significant improvement over the micro-rotation deconvolution. Our results suggest deconvolution of micro-rotation image series open some exciting new avenues for further analyses, ultimately laying the way towards establishing an enhanced resolution 3D light microscopy.

5. REFERENCES

[1] T. Schnelle, R. Hagedorm, G. Fuhr, S. Fielder, and T. Muller, "Three-dimensional electric field traps for manipulation of cells - calculation and experimental verification," *Biochemica et Biophysica Acta*, vol. 1157, pp. 127–140, 1993.

[2] O. Renaud, J. Vina, Y. Yu, C. Machu, A. Trouvé, H. Van der Voort, B. Chalmond, and S.L. Shorte, "High-resolution imaging of living cells in flow suspension using axial-tomography : 3d imaging flow cytometry," *Biotechnology J.*, vol. 3, no. 1, pp. 53–62, 2008.

[3] R. Lizundia, L. Sengmanivong, J. Guergnon, T. Muller, T. Schnelle, G. Langsley, and S.L. Shorte, "Use of micro-rotation imaging to study jnk-mediated cell survival in theileria parva-infected b-lymphocytes," *Parasitology*, vol. 130, pp. 629–635, 2005.

[4] S.L. Shorte, T. Muller, and T. Schnelle, *Method and device for 3 dimensional imaging of suspended micro-objects providing high-resolution microscopy*, Patent International Application No.PCT/EP2003/011818, 2003.

[5] Y. Yu, A. Trouvé, and B. Chalmond, "A bayesian 3d volume reconstruction for confocal micro-rotation cell imaging," in *Medical Image Computing and Computer-Assisted Intervention - Proc. of MICCAI 2007*, N. Ayache, S. Ourselin, and A. Maeder, Eds., october 2007, pp. 685–692.

[6] A.P. Dempster, N. Laird, and D.B. Rubin, "Maximum likelihood from incomplete data via the em algorithm," *Journal of the Royal Statistical Society, Series B*, vol. 39, pp. 1–38, 1977.

[7] L. A. Shepp and Y. Vardi, "Maximum likelihood reconstruction in positron emission tomography," *IEEE Trans. on Medical Imaging*, vol. 1, pp. 113–122, 1982.

[8] W.H. Richardson, "Bayesian-based iterative method of image restoration," *Journal of the Optical Society of America*, vol. 62, pp. 55–59, 1972.

[9] L. Lucy, "An iterative technique for the rectification of observed distributions," *Astronomical Journal*, vol. 79, pp. 745–754, june 1974.

[10] B. Chalmond, *Modeling and Inverse Problems in Image Analysis*, 2003.

[11] H. Hudson and R. Larkin, "Accelerated image reconstruction using ordered subsets of projection data," *IEEE Transactions on Medical Imaging*, vol. 13, no. 4, pp. 601–609, 1994.

[12] T. Chan and J. Shen, *Image Processing and Analysis*, 2005.

[13] N. Dey, L. Blanc-Féraud, C. Zimmer, Z. Kam, P. Roux, J.C. Olivo-Marin, and J. Zerubia, "Richardson-lucy algorithm with total variation regularization for 3d confocal microscope deconvolution," *Microscopy Research Technique*, vol. 69, pp. 260–266, 2006.